Drying Technology

ISSN: 0737-3937 (Print) 1532-2300 (Online) Journal homepage: https://www.tandfonline.com/loi/ldrt20

Impingement Heat Transfer for a Cluster of Laminar Impinging Jets Issuing from Noncircular Nozzles

Wennan Zhao , Kuruchi Kumar & Arun S. Mujumdar

To cite this article: Wennan Zhao , Kuruchi Kumar & Arun S. Mujumdar (2005) Impingement Heat Transfer for a Cluster of Laminar Impinging Jets Issuing from Noncircular Nozzles, Drying Technology, 23:1-2, 105-130, DOI: 10.1081/DRT-200047877

To link to this article: https://doi.org/10.1081/DRT-200047877

Published online: 16 Feb 2007.

Drying Technology, 23: 105–130, 2005

ISSN: 0737-3937 print/1532-2300 online
DOI: 10.1081/DRT-200047877

Taylor & Francis
Taylor & Francis Group

Impingement Heat Transfer for a Cluster of Laminar Impinging Jets Issuing from Noncircular Nozzles

Wennan Zhao and Kuruchi Kumar
Institute of High Performance Computing, Science Park, Singapore

Arun S. Mujumdar*
Department of Mechanical Engineering, National University of Singapore, Singapore

Abstract: Results of numerical simulation of the flow and heat transfer characteristics for a semi-confined cluster of laminar air jets impinging normally on a plane wall are presented. A central jet is surrounded by four equally spaced jets of the same configuration. Both circular and noncircular nozzles are considered. The nozzle footprint is displayed in the static pressure, temperature, and local Nusselt number contours on the impingement surface only for relatively short nozzle-to-surface distances. The heat transfer characteristics and performance of circular and noncircular nozzles are compared. It is observed that the Nusselt number based on property values at the jet temperature is relatively insensitive to the temperature difference between the jet and the impingement surface. Also, the local Nusselt numbers are independent of the thermal boundary condition; i.e., the values are nearly the same for both isothermal and uniform heat flux conditions at the target surface. Finally, Nusselt numbers for a single equivalent jet *viz*. one with the same area as the five nozzles in the cluster combined, are compared for the case of the circular jet.

Keywords: Cluster jets; Elliptic nozzle; Heat transfer; Noncircular jet; Nusselt number; Rectangular nozzle; Square nozzle; Thermal boundary conditions

*Correspondence: Arun S. Mujumdar; Fax: 65-6779-1459; E-mail: mpeasm@nus.edu.sg

INTRODUCTION

Impinging jets are widely and successfully used in numerous mass and heat transport applications requiring efficient drying, cooling, and heating. Due to the extensive industrial applications of impinging jets, numerous investigations have been conducted to study the heat transfer characteristics of impinging jets of various configurations through experiments and numerical simulations. The flow structure and heat transfer performance of impinging jets has been examined and reviewed by Goldstein and Franchett,[1] Martin,[2] Jambunathan et al.,[3] Viskanta et al.,[4] and Polat.[5] These comprehensive reviews have dealt with the effects of the jet Reynolds number, large temperature difference, cross-flow effects, nozzle-to-plate spacing, nozzle geometry, cross flow, jet inclination, and so on. Polat et al.[6] have provided a critical review of numerical simulation of various transport problems under impinging jets. Mujumdar and Huang[7] have discussed the selection of impingent nozzle configuration and the effects of key parameters of interest in the design of impingement dryers.

In the study of impinging jet, the issue of large temperature differences is important in many industrial applications such as paper drying and turbine blade cooling. For such cases, the temperature-dependance of thermophysical properties of the fluid must be considered. Few studies have been conducted so far on the effect of the large temperature differences in impinging jet flows due to the shortcomings of the experimental techniques. More recently Milosavljevic and Heikkilä[8] carried out an experimental investigation of impingement heat transfer at large jet air temperatures ranging from 100 to 700°C. The effect of large temperature differences on local Nusselt number under turbulent slot impinging jet has been studied numerically by Shi et al.[9] Their results indicate that small temperature differences show only minor differences between the local Nusselt numbers calculated using fluid thermal conductivity values evaluated at the jet, film, and wall temperature. However, large temperature differences (over 100°C) can result in significant differences between these three possible values of the local Nusselt numbers. The work of Shi et al.[10,11] on the effect of the fluid Prandtl number on impingement heat transfer is also relevant here since a large change in temperature also affects the fluid Prandtl number.

Noncircular jets have been identified as an efficient technique for passive flow control of heat transfer that allows significant improvement of the thermal performance in various practical systems at a relatively low cost because noncircular jets rely solely on changes in the geometry of the nozzle. Gutmark and Grinstein[12] reviewed the literature on the flow field under several different noncircular jet geometries and the pertinent physical mechanisms that control their development. Several issues

were common to all noncircular shapes; they included axis switching and the azimuthal variation of the shear-layer spreading rate and turbulence production. Clearly these will affect heat transfer in the turbulent regime. However, this work is confined to laminar regime.

It is understood that a single impinging jet yields a high heat transfer rate in the stagnation zone, which fades very rapidly within distance away from the impinging zone. Therefore, in order to obtain a more uniform distribution of the heat transfer coefficient and also cover the large areas encountered in practice, it is necessary to use jet arrays in industrial applications. A novel cluster of impinging jets is studied here in order to investigate the effect of jet–jet interaction that occurs in such an array and the resulting heat transfer distribution.

In this article, we present the predicted flow and heat transfer results for a cluster of laminar impinging jets, which may be circular or noncircular. The effects of small and large temperature differences between the jet and the impingement surface was studied with the consideration of the change of thermophysical properties. Moreover, the average Nusselt numbers for a single equivalent circular jet, *viz*. one with the same area as that of the five circular nozzles in the cluster, are also determined for a comparative evaluation.

NUMERICAL MODEL

Figure 1 shows schematically the flow configuration modeled. The laminar jets impinge perpendicularly onto a flat surface at a distance H from the nozzle plate. The airflow is assumed to be steady, laminar, and incompressible. The physical and thermal properties of the fluid are allowed to vary with temperature. The fluid is Newtonian (air).

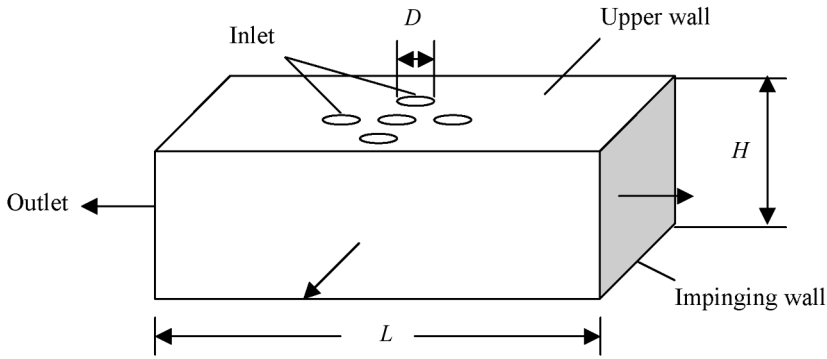

Figure 1. Schematic diagram of impinging jet geometry.

The set of equations for conservation of mass, momentum, and energy is solved to obtain the flow pattern and heat transfer distribution for the impinging jets. The well-known commercial CFD software (FLUENT, Version 6 [13]) was used to conduct the simulations. The equations solved are as follows:

$$\text{Mass balance: } \frac{\partial \rho}{\partial t} + \nabla \bullet \left(\rho \vec{v}\right) = 0 \tag{1}$$

Momentum balance:

$$\frac{\partial}{\partial t}\left(\rho \vec{v}\right) + \nabla \bullet \left(\rho \vec{v}\,\vec{v}\right) = -\nabla p + \nabla \bullet \left(\bar{\bar{\tau}}\right) + \rho \vec{g} + \vec{F} \tag{2}$$

$$\text{Energy balance: } \frac{\partial}{\partial t}(\rho E) + \nabla \bullet \left[\vec{v}(\rho E + p)\right] = \nabla \bullet (k \nabla T) \tag{3}$$

Due to the symmetry nature of the flow, only one quarter of the flow domain was simulated. The dimensions of the different noncircular nozzles are calculated based on the same cross area. The aspect ratios for both rectangular and elliptic jets were chosen to be 2. The full computational domain in the x and y direction has the same length of $35D$. The central jet is surrounded by four equally spaced jets of the same configuration. The distance between two adjacent nozzles is set at $5D$.

Uniform velocity profiles were specified at the nozzle exit. The confinement surface is assumed to be an adiabatic wall (well insulated). The target surface is either supplied with a constant heat flux or held at a constant temperature. Grid-independence tests were conducted in order to obtain suitable grid designing for the simulations. For instance, the grid-independence results for the case of square jet for $H/D = 1$, $X/D = 5$ with $Re = 500$ is shown in Fig. 2. It is clear that the difference between the local Nusselt numbers for the three different grids 99*99*40, 99*99*50, and 137*137*40 is very small (only 1.1% and 2.5%, respectively, at the maximum point). Thus the grid pattern of 99*99*40 was chosen to perform the calculations.

The local Nusselt number for an isothermal impingement surface is defined as:

$$Nu_x = \frac{h_x W}{\lambda} \tag{4}$$

where λ is the fluid thermal conductivity, and

$$h_x = q/\left(T_w - T_{ref}\right)$$

where W is the hydraulic diameter for the nozzles and T_{ref} is the reference temperature.

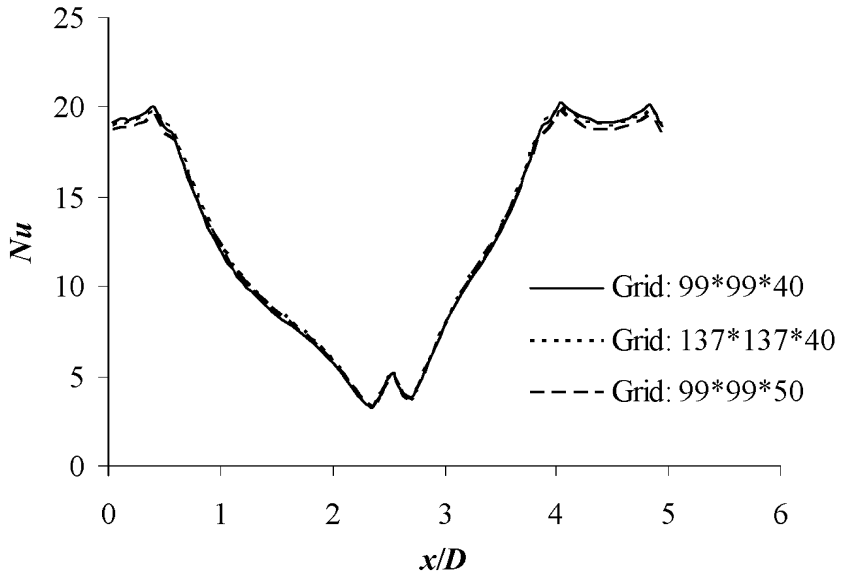

Figure 2. Grid-independence test for square jet ($Re = 500$, $H/D = 1$).

The fluid thermal conductivity can be calculated depending on the reference value selected. The most popular reference temperature is the film temperature, $T_f = (T_w - T_j)/2$. In this work, we calculated three Nusselt number values based on λ, at the jet temperature, the film temperature, and the impingement wall temperature. The corresponding Nusselt numbers are denoted by Nu_j, Nu_f, and Nu_w, respectively. A comparison is made between the Nusselt number distributions using these three definitions of Nu.

RESULTS AND DISCUSSION

Numerical investigations were carried out for the cluster of air impinging jets, both circular and noncircular. The distance between two adjacent jets was held constant at $5D$ and H/D was set at unity. Three different Reynolds numbers were used in the simulations, *viz*. 250, 500, and 1000. The Reynolds number is based on the hydraulic diameter, which is defined as: $D_h = 4A/P$, where A is the sectional area of the nozzle and P is the perimeter of the nozzle. Note that the nozzle open area and inter-nozzle spacing in the cluster were held constant to minimize the number of parameters in this exploratory study.

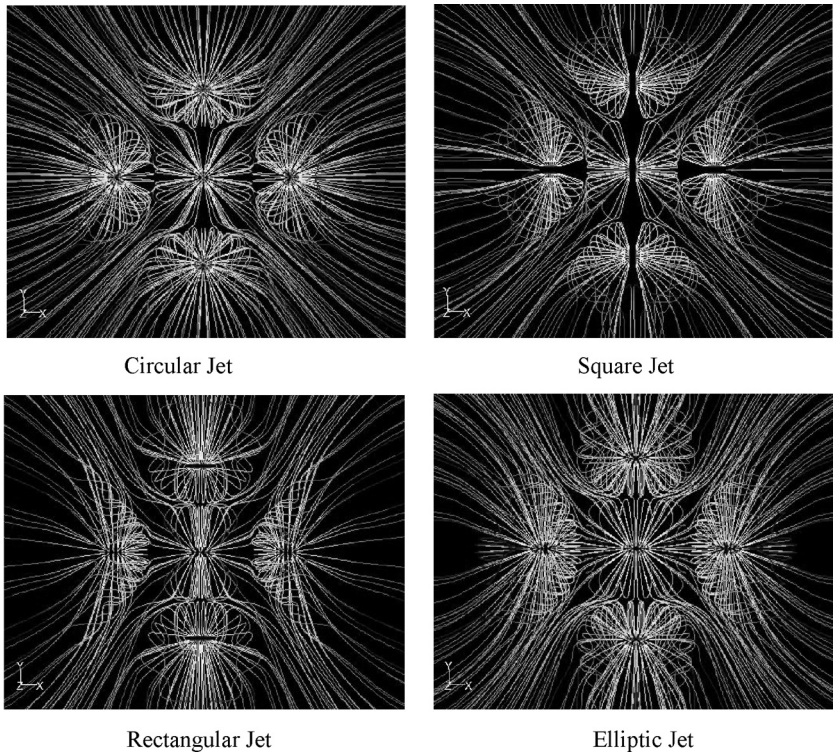

Figure 3. Projection of flow lines on the target surface for various impinging jets ($Re = 500$, $H/D = 1$).

Flow Patterns

Figure 3 shows projection of flow lines on the impingement surface for clusters of circular, square, rectangular, and elliptic jets. The Reynolds number in each case is 500. Similar to the impinging jet array, the heat transfer performance of the cluster of impinging jet is expected to be affected by the interference caused by adjacent jets before impingement. Jet interference occurs due to the shear layer expansion at the small jet-to-jet spacing used. It can be seen from Fig. 3 that the flow lines emanating from the central nozzle are affected by the surrounding four jets; the fluid from the central jet passes through the space between two adjacent jets. Clearly, as the inter-nozzle spacing is reduced, greater interaction will result between neighboring jets.

As expected, the flow line contours for circular and square jets are similar, while those for elliptic and rectangular jets are similar. As H/D

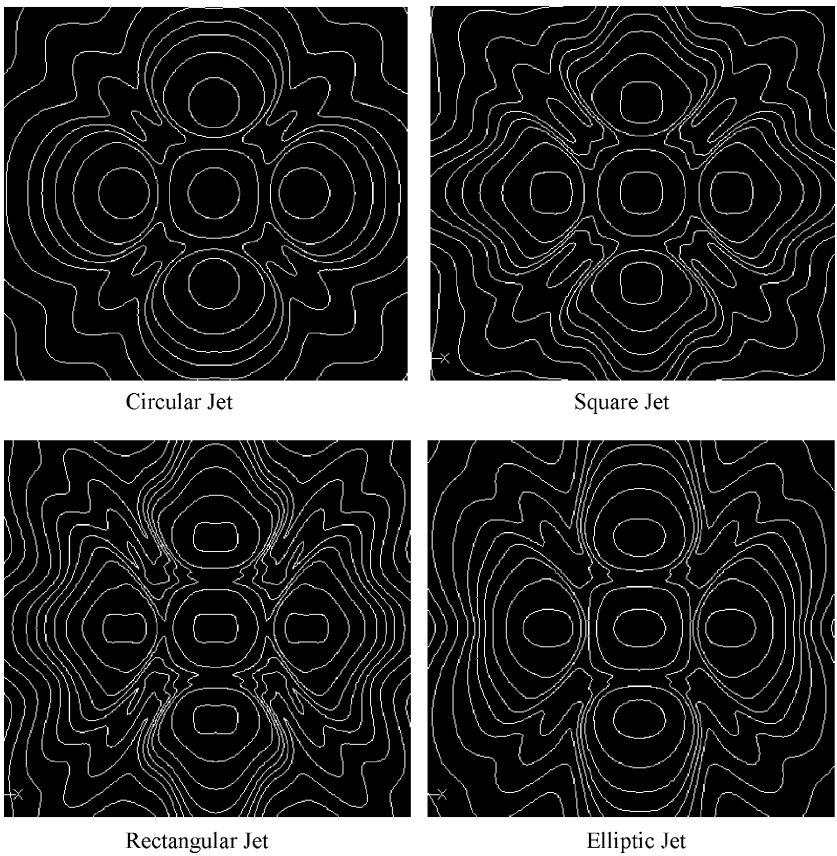

Figure 4. Contours of the static temperature on the target surface for various jets ($Re = 500$, $H/D = 1$).

increases the trend of the flow is toward achieving axisymmetry. Flow lines for all jets look similar at the target surface at larger H/D. This must also reflect in the local heat transfer distribution as well.

Typical contours of the temperature distribution on the impinging jet for the four nozzles are displayed in Fig. 4. Due to the small nozzle-to-plate distance ($H/D = 1$), the contours retain the shape of the orifices, although the trend toward axisymmetry is clearly evident.

The contours of static pressure on the impingement surface are displayed in Fig. 5 for both circular and noncircular jets. It is observed that the contour lines are much denser around the edges of the footprints of the orifices, which indicates the existence of the high-pressure gradient in this region.

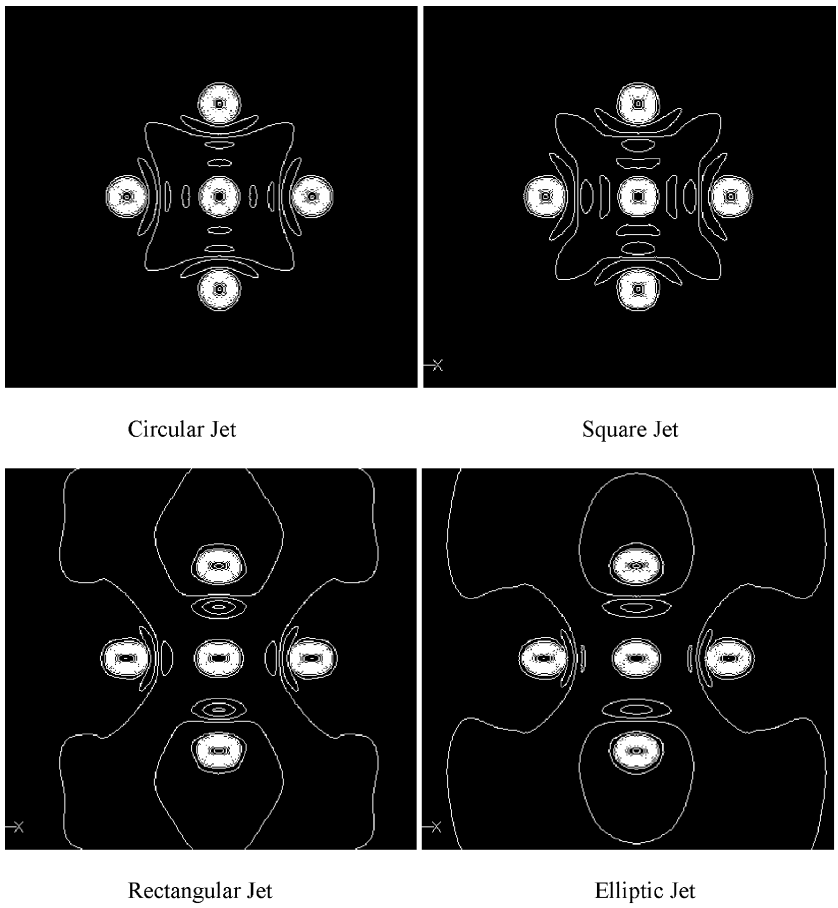

Figure 5. Contours of static pressure distributions on the impinging surface for various jets ($Re = 500$, $H/D = 1$).

It is clearly seen from Figs. 3–5 that, due to the symmetric geometric structure of the circular and square jets in x and y directions, the flow patterns for these two types of nozzles also show symmetry in these directions. With the aspect ratio of 2:1 for the rectangular and elliptic jets, the gap between the adjacent nozzles in the major axis direction is much shorter than that along the minor axis direction. Therefore, the flow lines on the major axis side are more distorted, which implies greater interaction of the jet flows between the adjacent nozzles in this direction. For the noncircular jets, mixing between the jet flow and the surroundings is enhanced, and the entrainment rate for the rectangular and elliptic jets

are much larger than those for circular jets, which will enhance their thermal performance in the impingement region.

Heat Transfer

The three-dimensional plots of the Nusselt number for the circular and noncircular nozzles are illustrated in Fig. 6. It is seen that there are four peaks at the four corners of the square and rectangular jets, and two peaks occur along the major axis of the elliptic jet. As expected, a high Nusselt number exists at the sharp corners of the corresponding projected area of the nozzles on the impinged surface. The existence of the peak Nusselt numbers is due to much higher jet velocities in the corner region, which has also been observed by Sfeir,[14] Tsuchiya et al.,[15] and Quinn[16] for a turbulent single rectangular impinging jet and by Sezai and Mohamad[17] for a laminar rectangular impinging jet with short distance from jet to the target wall. Sezai and Mohamad[17] observed that the impinging flow has strong vorticity near the impingement plate and that the vorticity weakens away from the impingement plate.

Effect of Reynolds Number

Simulations were carried out for three jet Reynolds numbers to study its effect on the performance of clusters of circular and noncircular jets at a spacing ratio of $H/D = 1$. Figures 7–10 show the local Nusselt number distributions along the line of symmetry passing through the main axes at three Reynolds numbers, *viz*. 250, 500, and 1000 for clusters of circular, square, rectangular, and elliptic jets. With increase of the Reynolds number, the local Nusselt number increased for both circular jets and noncircular jets cluster, especially in the stagnation region, which is due to the increase of momentum of the jet. The shape of the *Nu* distribution remained similar with several peaks and valleys. A small secondary peak is seen to appear between neighboring jets at higher Reynolds number due to enhanced interaction between jets. Possible negative effects of "spent flow" from adjacent jets is minimal as the jets are spaced sufficiently so that the spent flow can easily pass between the jets without interacting with them. Figure 3 shows that the rectangular jet is the best to alleviate the negative effects of spent flow. The asymmetric local Nusselt number distribution between the two nozzles along the axis can be observed in these figures, which would also be found in the following investigations. The asymmetric structure of the distribution can be contributed to the asymmetric boundary condition for the surrounding nozzles, since there are no more nozzles to be considered in the opposite direction of the central nozzle in the current study.

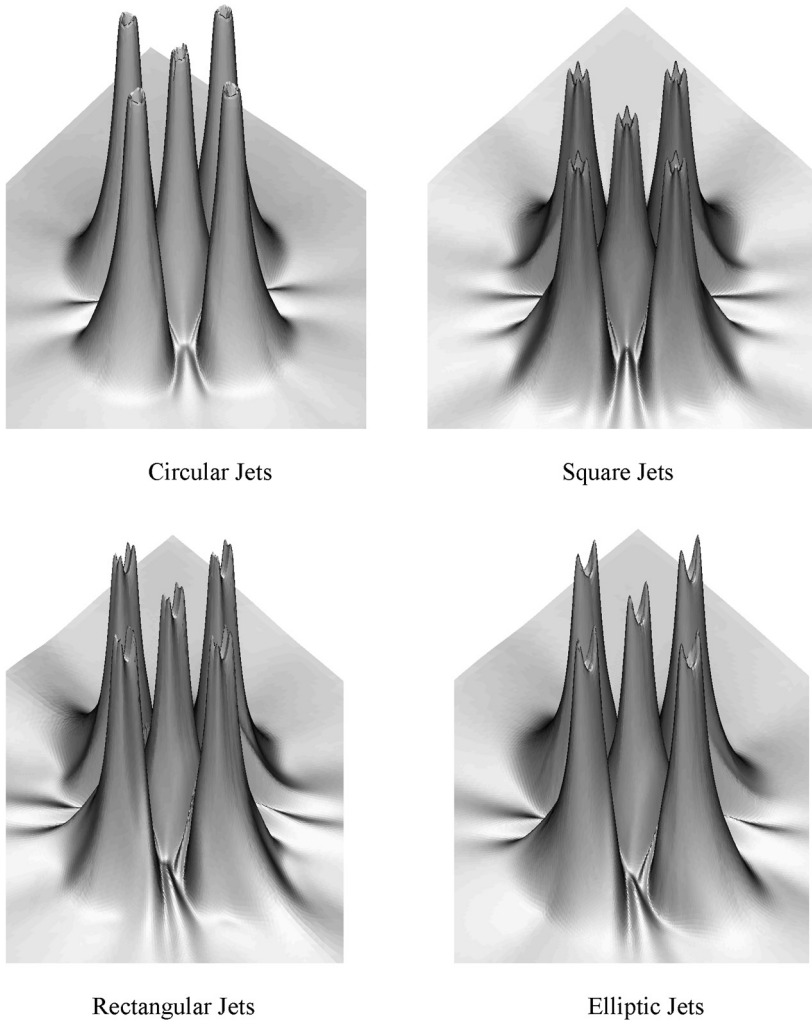

Figure 6. 3D plot of local Nusselt number distributions for circular and noncircular cluster jets.

Effect of Thermal Boundary Conditions

The effect of thermal boundary conditions on the Nusselt number was studied for both isothermal and uniform heat flux conditions at the target surface for all clusters. Three different thermal boundary conditions were investigated: constant wall temperature at 320 K and constant heat flux of $1\,kW/m^2$ and $0.5\,kW/m^2$. The Reynolds number is kept at 500 for all the cases. The effect of temperature dependence of the properties of

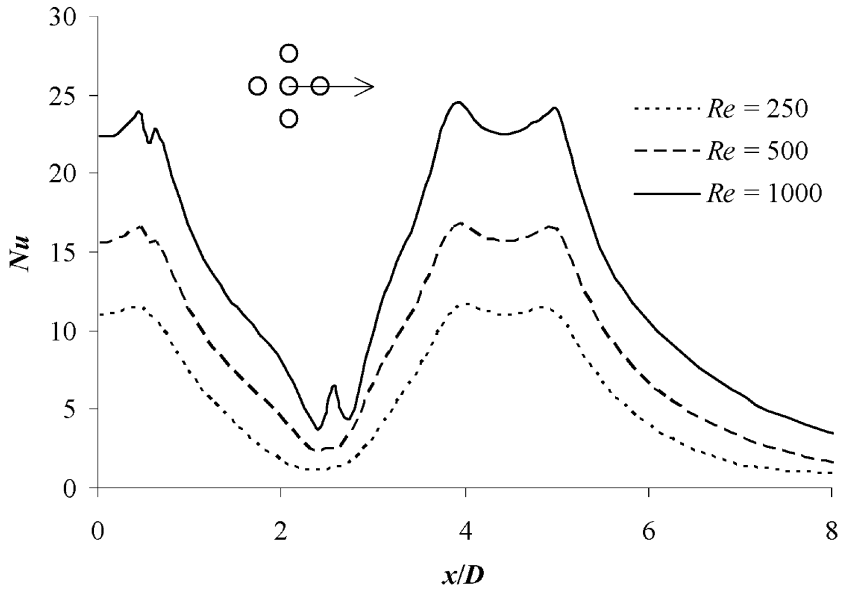

Figure 7. Local Nusselt number distributions along the axis at different Reynolds number for a cluster of circular jets.

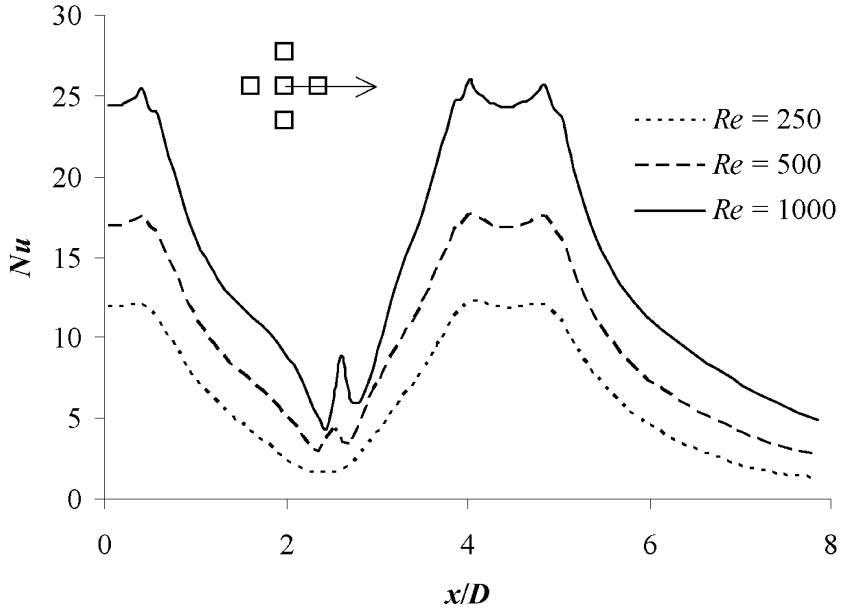

Figure 8. Local Nusselt number distributions along the axis at different Reynolds number for a cluster of square jets.

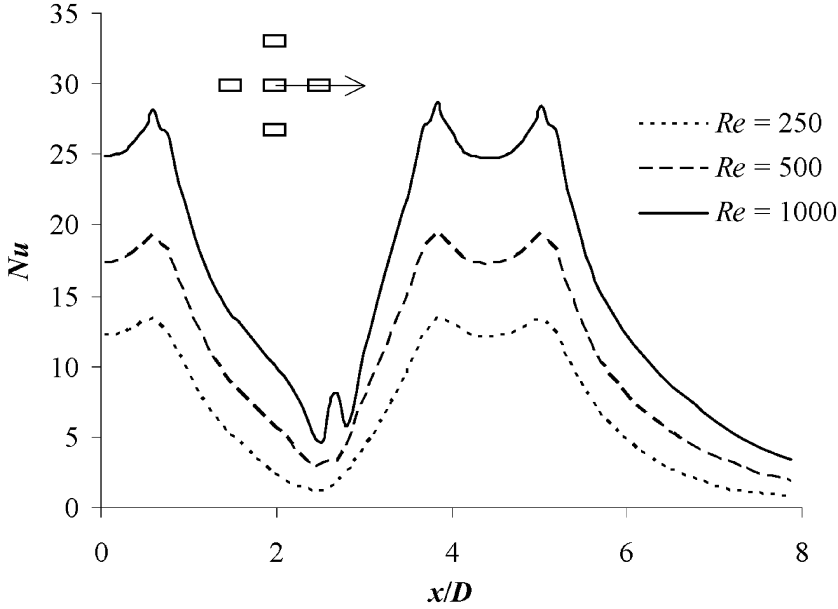

Figure 9. Local Nusselt number distributions along the major axis at different Reynolds number for a cluster of rectangular jets.

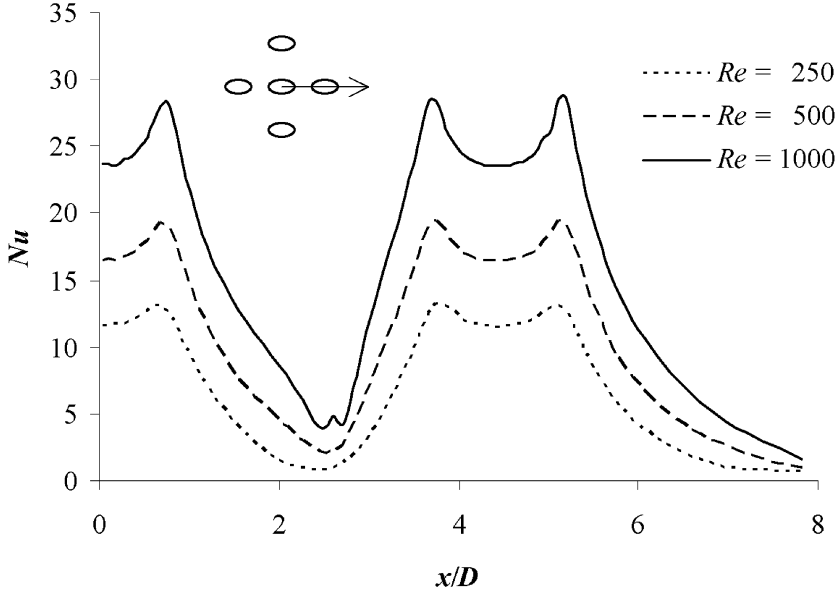

Figure 10. Local Nusselt number distributions along the major axis at different Reynolds number for a cluster of elliptic jets.

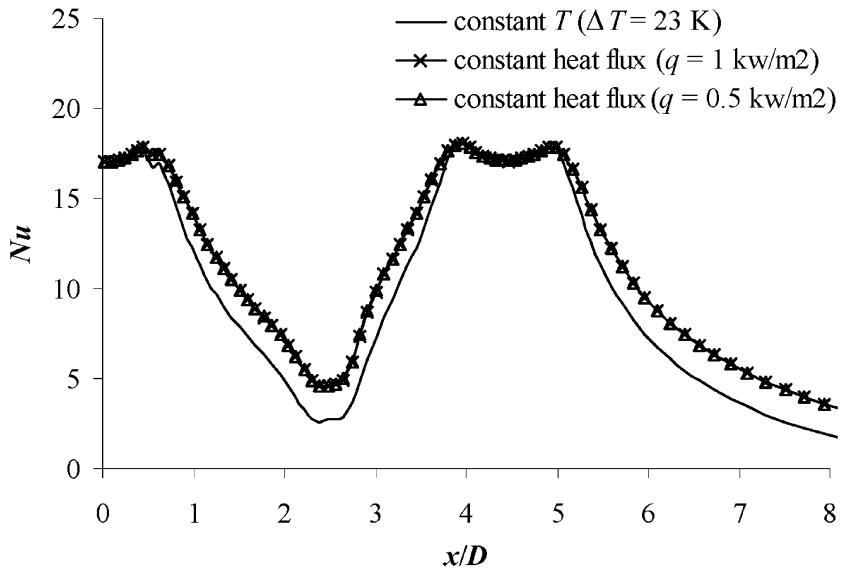

Figure 11. Local Nusselt number distributions along the axis for different thermal boundary conditions for the cluster circular jets.

the fluid was considered. The Nusselt number at the impingement surface along the major axis is shown in Figs. 11–14 for circular, square, rectangular, and elliptic jets, respectively.

It can be clearly seen from Figs. 11–14 that the local Nusselt number is nearly independent of the thermal boundary conditions. The Nusselt numbers are nearly the same even when the heat flux is doubled. The case of constant temperature shows slightly lower Nusselt number in the interaction area while not much difference in the stagnation area. This effect is possibly due to mixing of the spent flow with jet flow. The same trend is discerned for all four nozzles, *viz*. circular, square, rectangular, and elliptic jets. Increasing the heat flow further will likely introduce effects due to temperature-dependent fluid properties as shown in the next section.

Effect of Temperature Difference Between Nozzles and Target Surfaces

Circular Jets

Simulations at three temperature difference values between the jet fluid and the target surface were carried out to study its effect on the jet cluster performance with the constant Reynolds number at 500. Only the cooling

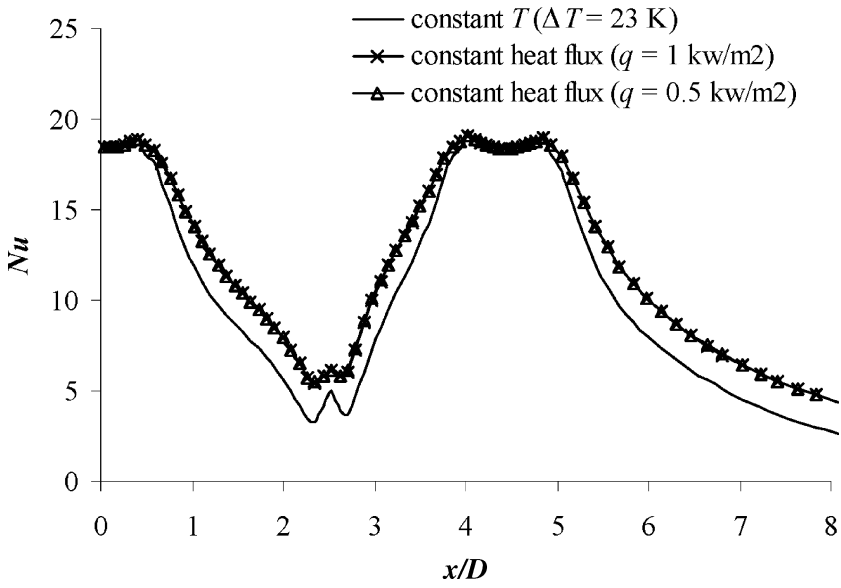

Figure 12. Local Nusselt number distributions along the axis for different thermal boundary conditions for the cluster square jets.

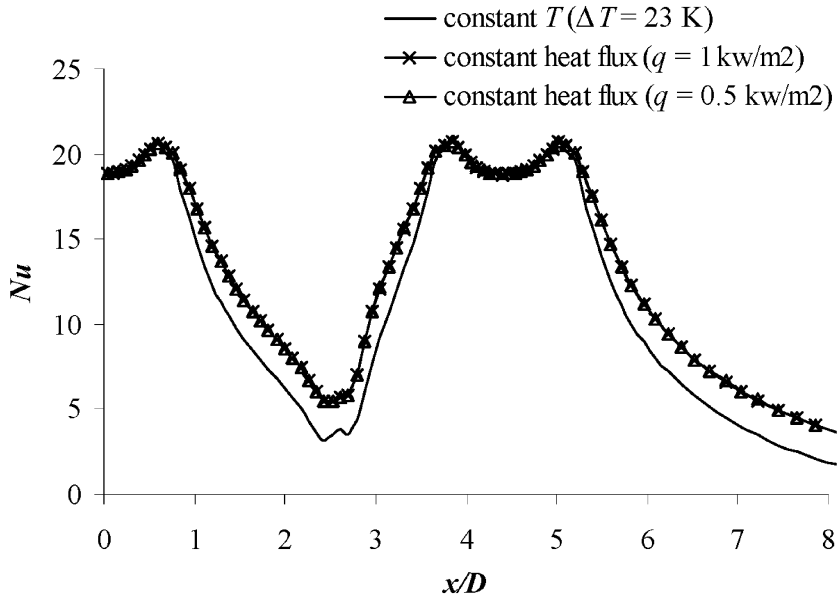

Figure 13. Local Nusselt number distributions along the major axis for different thermal boundary conditions for the cluster rectangular jets.

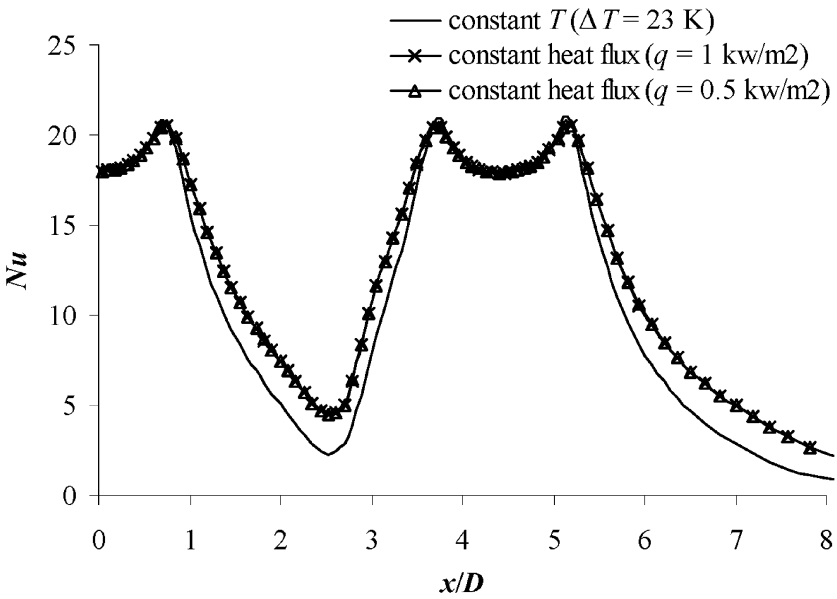

Figure 14. Local Nusselt number distributions along the major axis for different thermal boundary conditions for the cluster elliptic jets.

case was simulated, *viz*. the temperature of the target surface is higher than the fluid from the nozzle in this study. The three temperature difference values used were 23 K, 100 K, and 200 K, which may be considered as low, medium, and high temperature difference values.

In this work, the jet temperature, film temperature, and impingement wall temperature were used as reference temperatures to evaluate the fluid thermal conductivity, λ; the corresponding Nusselt numbers are denoted by Nu_j, Nu_f, and Nu_w, respectively. A comparison is made between the Nusselt number distributions computed under these three definitions. Figures 15–17 display the computed results of the local Nusselt number distribution for the cluster circular jets. Figure 15 shows that the Nusselt numbers based on jet temperature are less sensitive to the temperature difference than the other two. This result shows that, for design purpose, data taken at small temperature difference can be used to estimate the heat transfer coefficient if the jet temperature, rather than film or target temperature, is used as the reference temperature.

Noncircular Jets

The local Nusselt number distribution, which is based on the three definitions of *Nu*, are shown in Figs. 18–20 for square jets, in Figs. 21–23 for rectangular jets, and in Figs. 24–26 for elliptic jets; the Reynolds number

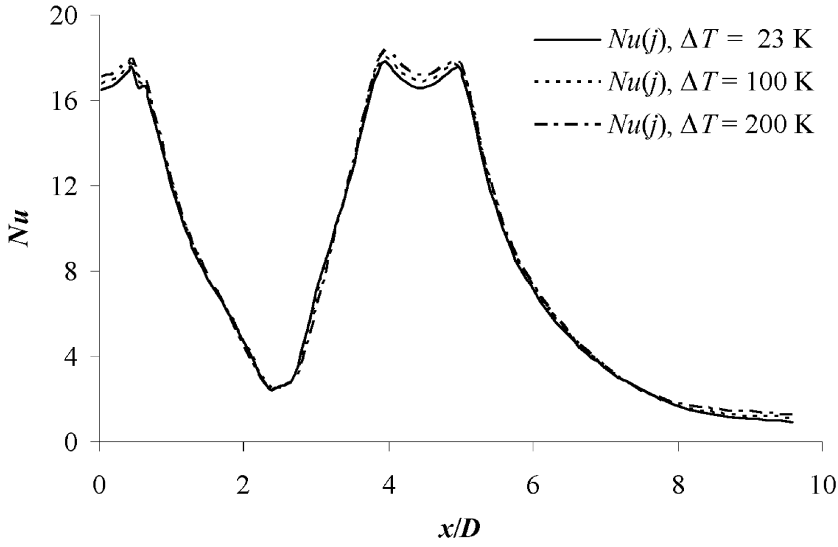

Figure 15. Local Nusselt number based on jet temperature along the axis for circular jets of air at different temperature differences.

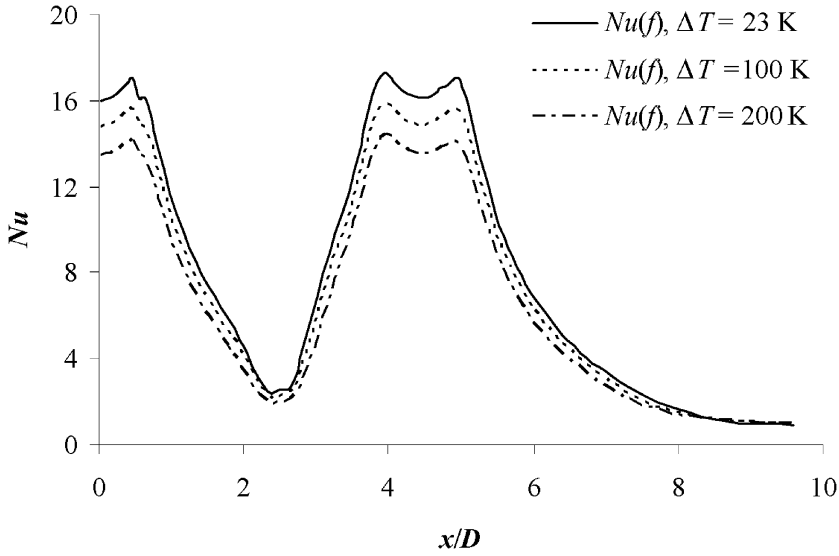

Figure 16. Local Nusselt number based on film temperature along the axis for circular jets of air at different temperature differences.

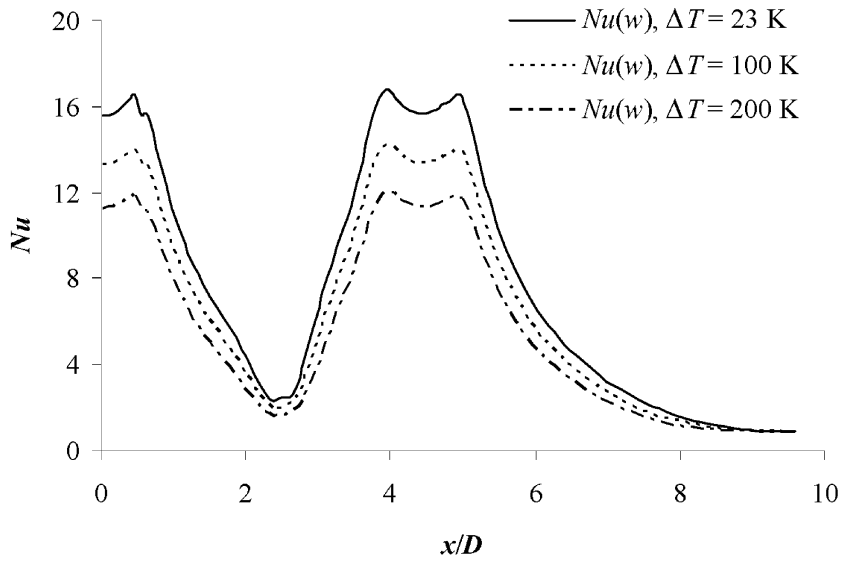

Figure 17. Local Nusselt number based on impingement wall temperature along the axis for circular jets of air at different temperature differences.

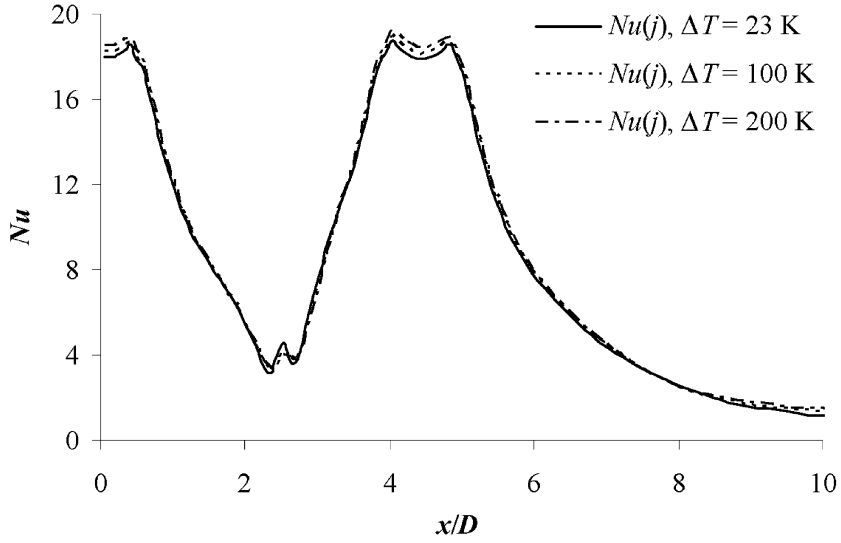

Figure 18. Local Nusselt number based on jet temperature along the axis for square jets of air at different temperature differences.

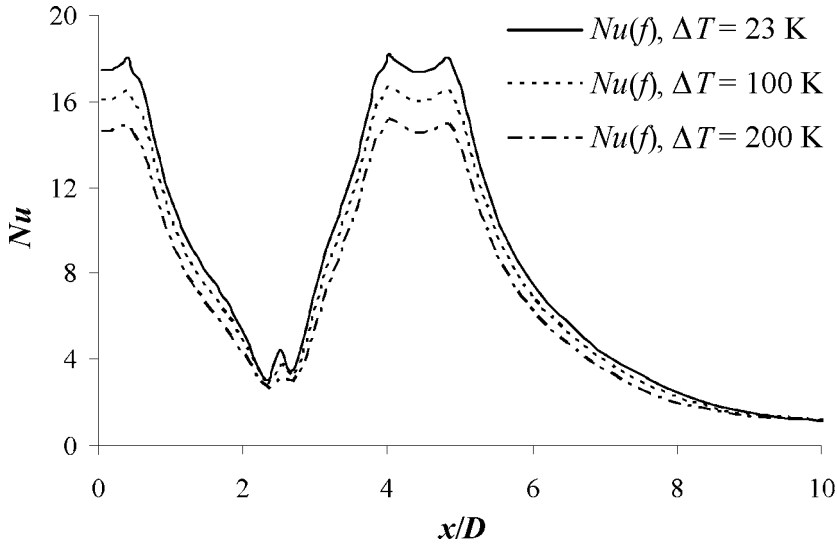

Figure 19. Local Nusselt number based on film temperature along the axis for square jets of air at different temperature differences.

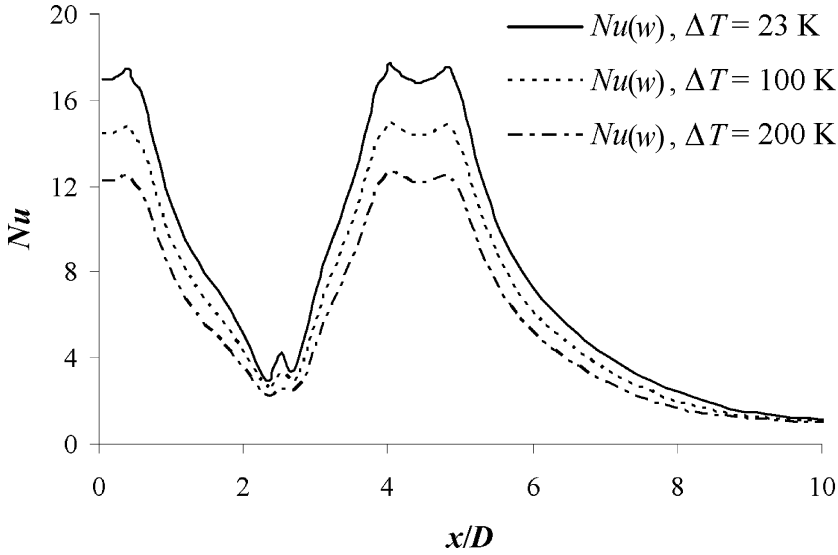

Figure 20. Local Nusselt number based on impingement wall temperature along the axis for square jets of air at different temperature differences.

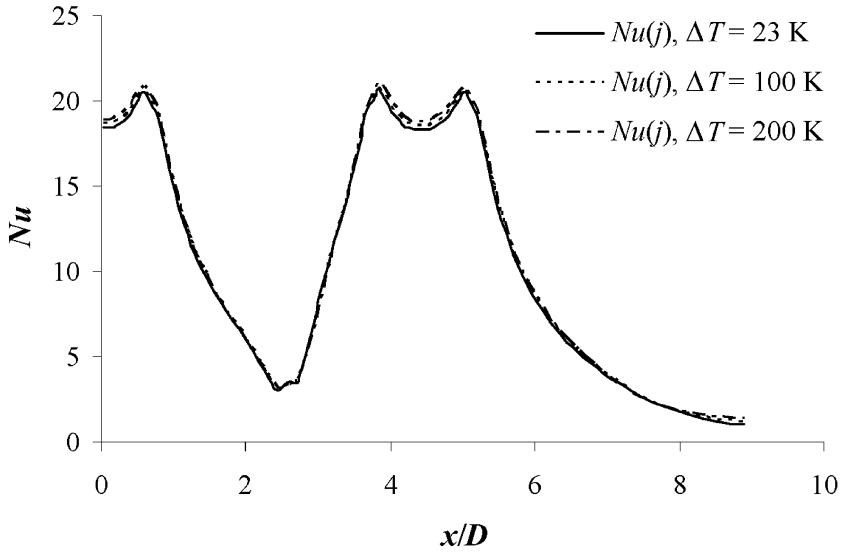

Figure 21. Local Nusselt number based on jet temperature along the major axis for rectangular jets of air at different temperature differences.

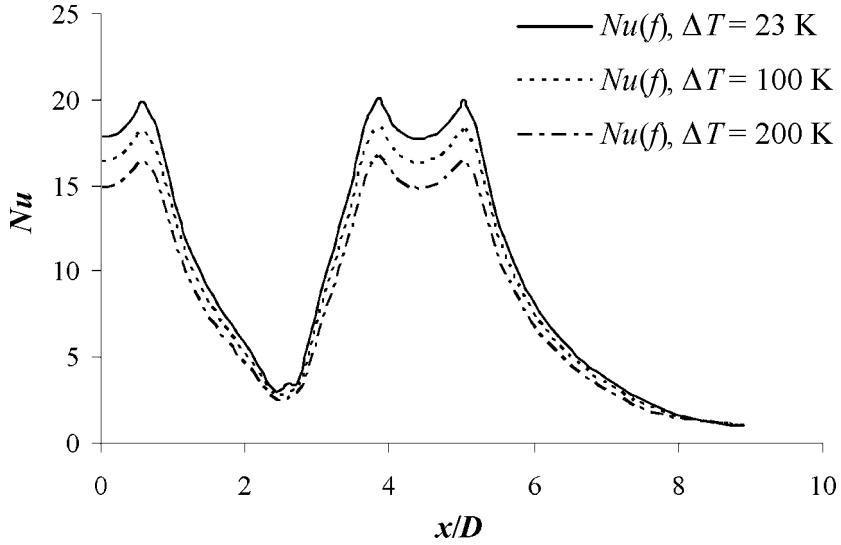

Figure 22. Local Nusselt number based on film temperature along the major axis for rectangular jets of air at different temperature differences.

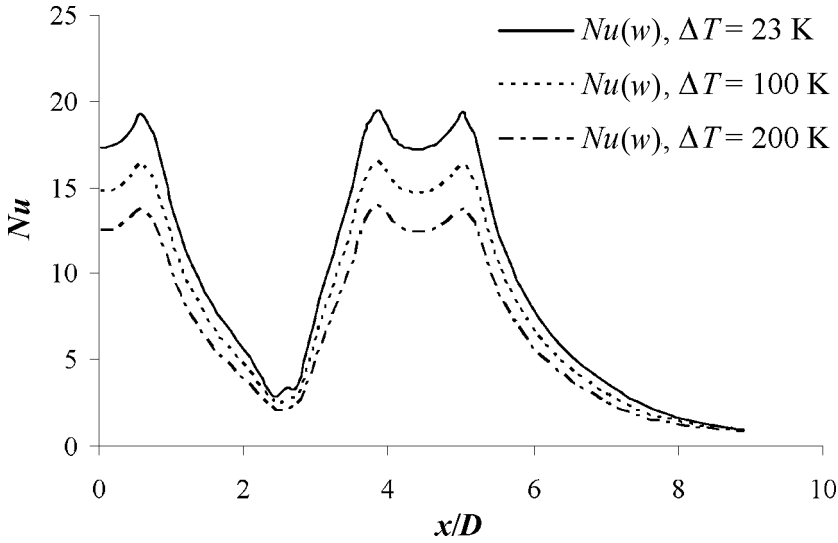

Figure 23. Local Nusselt number based on impingement wall temperature along the major axis for rectangular jets of air at different temperature differences.

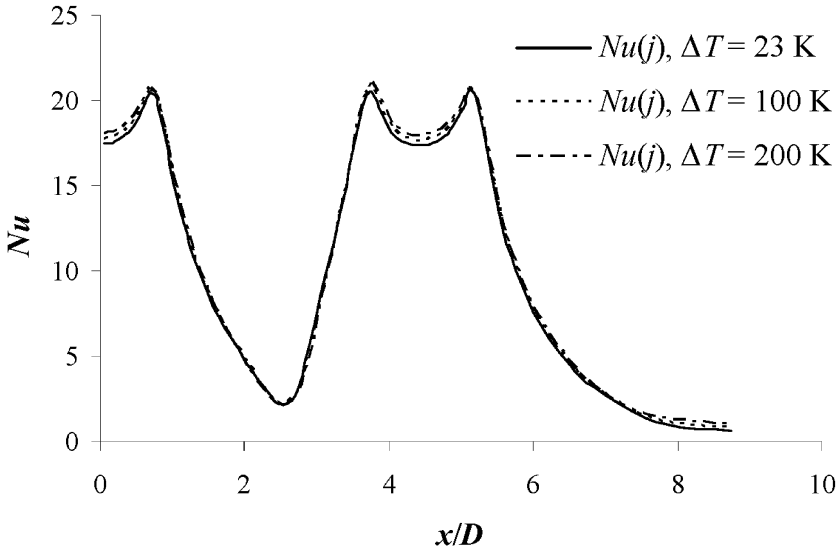

Figure 24. Local Nusselt number based on jet temperature along the major axis for elliptic jets of air at different temperature differences.

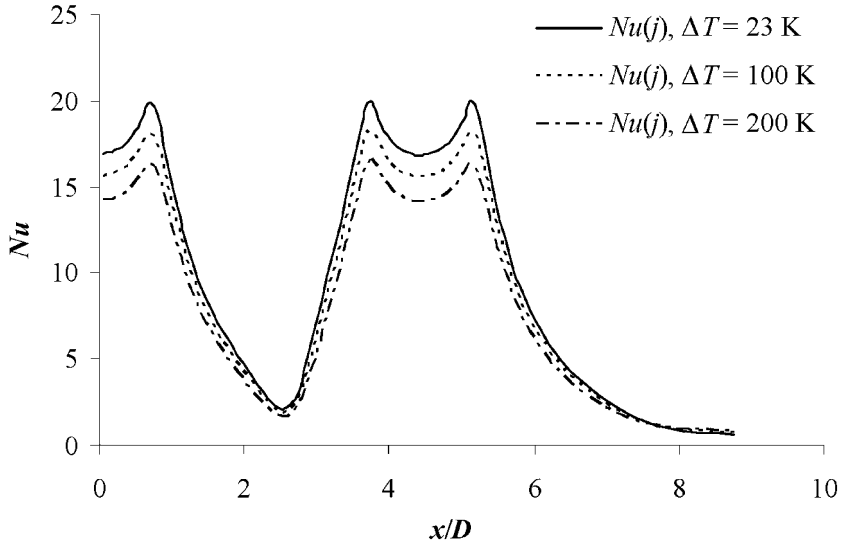

Figure 25. Local Nusselt number based on film temperature along the major axis for elliptic jets of air at different temperature differences.

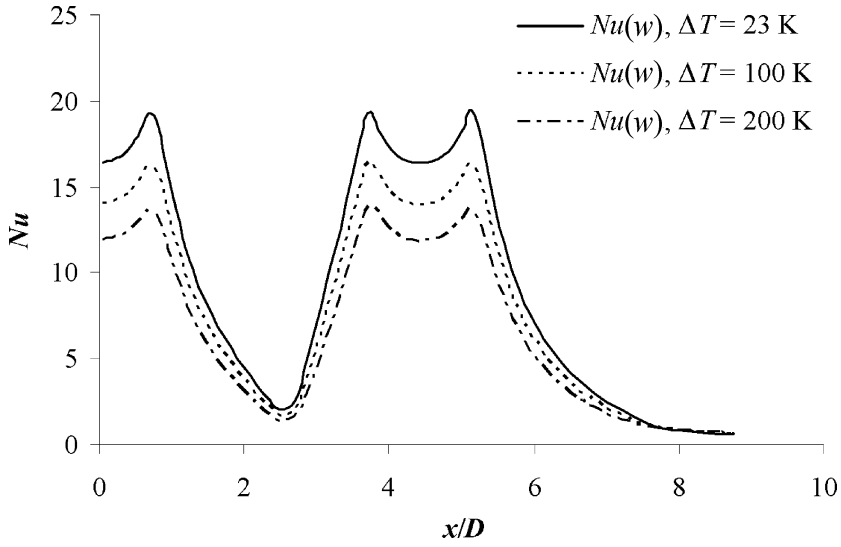

Figure 26. Local Nusselt number based on impingement wall temperature along the major axis for elliptic jets of air at different temperature differences.

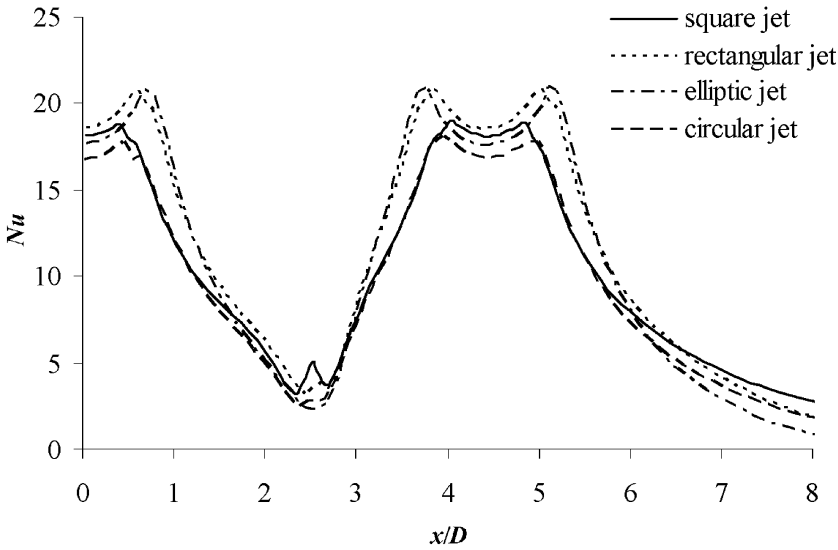

Figure 27. Local Nusselt number distributions along the major axis for different nozzles.

is kept unchanged as 500. These results show that for small temperature differences only minor differences exist between the local Nusselt numbers calculated using the three reference temperatures. However, large temperature differences (over 100°C) can result in significant differences between the values of the three possible definitions of the Nusselt numbers. Interestingly, the results shown here for noncircular jets and their clusters are similar to those of Shi et al.[9] for a turbulent slot impinging jet.

Comparison of Heat Transfer Performance of Different Jets

All four types of nozzles are compared for their heat transfer performance under the same operating conditions. The temperature difference between the fluid from the nozzle and the target surface is kept constant at 23 K and the Reynolds number is 500. Figure 27 shows the local Nusselt number distribution for the four cluster nozzles along the major axis. The local Nusselt number distributions of circular jets and square jets are quite similar. The same observation applies to rectangular and elliptic jets. It is confirmed that the flow pattern and the local heat transfer distribution reflect the same trend. Generally the local Nusselt numbers for rectangular jets and elliptic jets are higher than those for the circular and square jets, which is due to the enhanced entrainment, especially in the impingement zone.

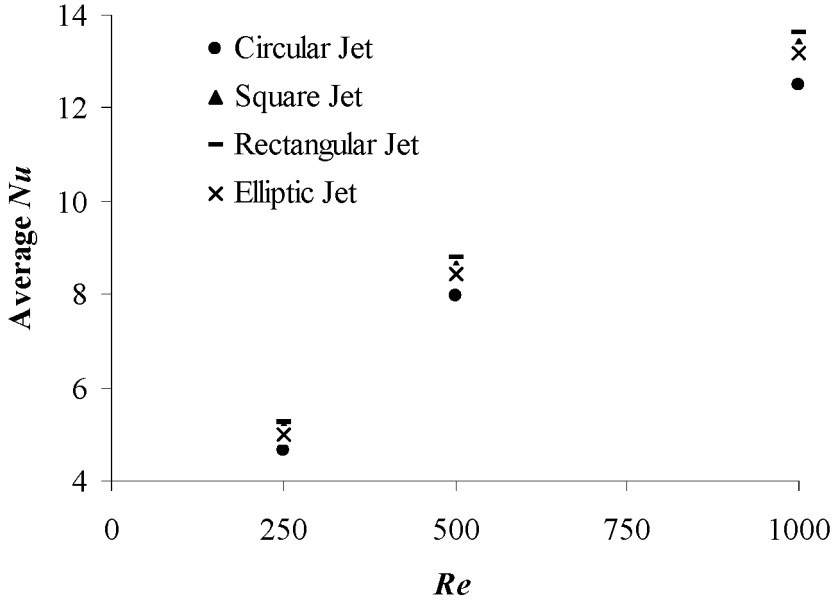

Figure 28. Comparison of the average Nusselt number distributions for different nozzles.

The average Nusselt number for the cluster circular and noncircular jets at various Reynolds number are compared for a selected averaging area. A comparison of the surface-averaged Nusselt number is displayed in Fig. 28. The heat transfer performance of the rectangular jets is better than that of the others at all three Reynolds numbers. In contrast, cluster circular jets give the worst performance. In summary, for low jet-to-plate spacings in laminar region a cluster of noncircular jets offers higher average Nusselt numbers than an equivalent cluster of circular jets. This can be explained as a result of the off-center velocity peaks downstream of the noncircular nozzles, which cause off-center peaks in the Nusselt number, clearly shown in Fig. 6. At large spacings, the difference between the various jet geometries will diminish, and even totally vanish. Hence, this study was confined only to closer spacing between the jet nozzle and impingement plate.

Comparison of Performance of Single and Cluster Circular Jets

The heat transfer performance of the cluster circular of jets was compared with a single "equivalent" circular jet. The single circular jet has the same area as that of the total area of the 5 nozzles in the cluster. The inlet velocity is kept the same for the two cases.

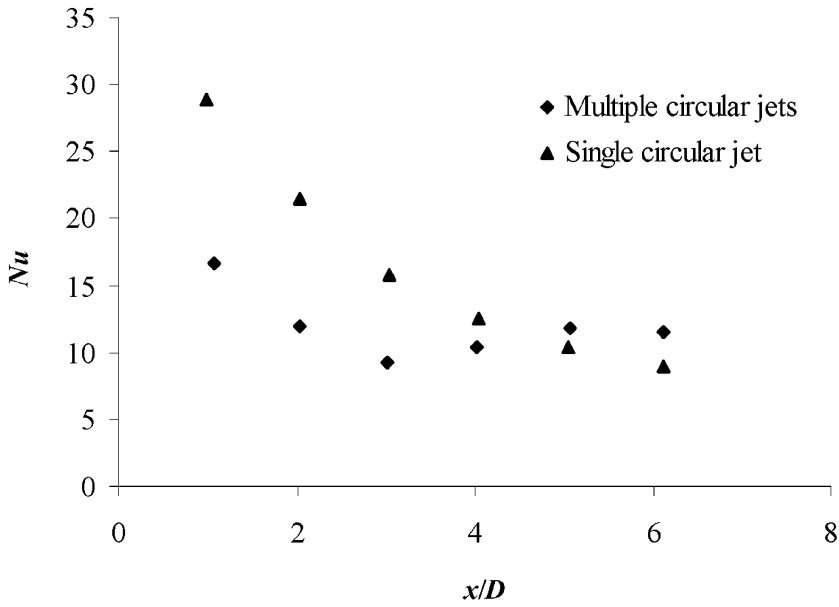

Figure 29. Comparison of the average Nusselt number for single and cluster circular jets.

Figure 29 displays the heat transfer performance comparison of average Nusselt number distributions for single and equivalent cluster circular jets. The heat transfer rate for a single jet in the central area is much higher than that of the jet cluster, but the profile drops sharply away from the stagnation region; the cluster jets perform better than the single jet beyond $r = 4D$. It is evident that cluster jets offer a relatively uniform local Nusselt number. Therefore, cluster jets can be used instead of single jet when a relatively uniform local Nusselt number is required in a certain area with small peak-to-valley variation. Similar results may be expected from noncircular clusters, *viz*. greater uniformity of Nusselt number away from the stagnation region of the central jet.

CONCLUSIONS

The flow and heat transfer characteristics of a semi-confined cluster of laminar jets impinging normally on a plane wall are presented for both circular and noncircular nozzles. The heat transfer performance of the four types of nozzles are compared. The effect of jet fluid and target surface temperature difference on the local Nusselt number was also

studied. Further, a single circular nozzle, which has the same area and same Reynolds number as the cluster of five circular jets, is simulated to compare the performance of the single and equivalent cluster jets. The following conclusions are valid over the parameter ranges investigated.

1. At small nozzle-to-plate distances, the contours of temperature and static pressure on the impingement wall reflect the geometry of the nozzles.
2. The local Nusselt number distributions of circular jets and square jets are similar, while those of rectangular jets and elliptic jets are similar. The average Nusselt number of rectangular jets shows the best performance at low jet-to-plate spacings and Reynolds number, while the cluster circular jets offer the lowest Nusselt number among the nozzles studied.
3. The Nusselt number based on jet temperature is found to be relatively insensitive to the temperature difference between the jet and the impingement surface. Also, the local Nusselt numbers are nearly independent of the thermal boundary condition; i.e., the values are nearly the same for both isothermal and uniform heat flux conditions at the target surface.
4. Although the heat transfer performance of an equivalent single jet is higher in the central area, the cluster nozzles can be used instead of single jet where a relatively uniform local Nusselt number is required. More studies are needed to determine the optimal spacing between jets as well as the number of jets in a single cluster.

NOMENCLATURE

A	section area of the nozzle, m^2
D	equivalent diameter of nozzles, m
h	surface heat transfer coefficient, $W \cdot m^{-2} \cdot K^{-1}$
H	nozzle-to-plate spacing, m
L	length of the confinement and impingement walls, m
Nu	Nusselt number
P	perimeter of the nozzle, m
q	heat flux, $W \cdot m^{-2}$
Re	Reynolds number
U, V	velocity in x, y direction, $m \cdot s^{-1}$
W	nozzle width, m
X	distance between the adjacent nozzles, m
x	distance away from the origin of the coordinates, m
λ	thermal conductivity, $W \cdot m^{-1} \cdot K^{-1}$

Subscripts

j	inlet condition
f	film condition
w	impingement wall

REFERENCES

1. Goldstein, R.J.; Franchett, M.E. Heat transfer from a flat surface to an oblique impinging jet. Trans. ASME, Journal of Heat Transfer **1988**, *110*, 84–90.
2. Martin, H. Heat and mass transfer between gas jets and solid surfaces. Advances in Heat Transfer **1977**, *13*, 1–60.
3. Jambunathan, K.; Lai, E.; Moss, M.A.; Button, B.L. A review of heat transfer data for single circular jet impingement. International Journal of Heat and Fluid Flow **1992**, *13*, 106–115.
4. Viskanta, R. Heat transfer to impinging isothermal gas and flame jets. Experimental Thermal and Fluid Science **1993**, *6*, 111–134.
5. Polat, S. Heat and mass transfer in impingement drying. Drying Technology **1993**, *11* (6), 1147–1176.
6. Polat, S.; Huang, B.; Mujumdar; A.S.; Douglas, W.J.M. Numerical flow and heat transfer under impinging jets: A review. Annual Review of Numerical Fluid Mechanics and Heat Transfer **1989**, *2*, 157–197.
7. Mujumdar, A.S.; Huang, B. Impingement Dryers. In *Handbook of Industrial Drying Vol. 2;* Mujumdar, A.S., Ed.; Marcel Dekker: New York, 1995.
8. Milosavljevic, N.; Heikkilä, P. Investigation of impingement heat transfer coefficient at high temperatures. Drying Technology **2002**, *20* (1), 211–222.
9. Shi, Y.L.; Ray, M.B.; Mujumdar, A.S. Effect of large temperature differences on local Nusselt number under turbulent slot impingement jet. Drying Technology **2002**, *20*, 1803–1825.
10. Shi, Y.; Ray, M.B.; Mujumdar, A.S. Effect of Prandtl number on impinging jet heat transfer under a semi-confined turbulent slot jet. International Communications in Heat and Mass Transfer **2002**, *29* (7), 929–938.
11. Shi, Y.; Ray, M.B.; Mujumdar, A.S. Effect of Prandtl number on impinging jet heat transfer under a semi-confined laminar slot jet. International Communications in Heat and Mass Transfer **2003**, *30* (4), 455–464.
12. Gutmark, E.J.; Grinstein, F.F. Flow control with noncircular jets, Annual Review of Fluid Mechanics **1999**, *31*, 239–272.
13. Fluent 6.0 User Guide, Fluent Inc., 2001.
14. Sfeir, A. Investigation of three-dimensional turbulent rectangular jets. AIAA Journal **1979**, *17*, 1055–1060.
15. Tsuchiya, Y.; Horikoshi, C.; Sato, T. On the spread of rectangular jets. Expermental Fluids **1986**, *4*, 1197–1204.
16. Quinn, W.R. Passive near-field mixing enhancement in rectangular jet flows. AIAA Journal **1991**, *29*, 515–519.
17. Sezai, I.; Mohamad, A.A. 3-D Simulation of laminar rectangular impinging jets, flow structure and heat transfer. ASME Journal of Heat Transfer **1999**, *121*, 50–56.